

MEDIUM FIELD Q-SLOPE STUDIES IN QUARTER WAVE CAVITIES

A. Grassellino, K. Fong, R.E. Laxdal, B. Waraich, V. Zvyagintsev (TRIUMF, Vancouver)

Abstract

The quality factor of superconducting radio-frequency niobium cavities decreases with the applied RF field in the medium field range. The medium field Q-slope effect has been investigated by many authors but models, most commonly including thermal feedback, do not fully explain experimental evidence. In this contribution we analyze medium field Q-slope data measured on ISAC-II low beta quarter wave cavities. The investigation takes the direction of testing the thermal dependence of the medium field Q-slope. Two surface heaters are added on the LHe side of the cavity in the high magnetic field region and Q-curves are acquired at different heater power levels. The data is then compared with a model that, in addition to thermal feedback of the surface temperature, takes into account the reduction of the critical temperature with the applied magnetic field. We then draw conclusions concerning the thermal feedback mechanism and on the relationship between the critical temperature field dependence and the Q-slope.

INTRODUCTION

A typical plot of a cavity quality factor as a function of the peak magnetic field B_p shows a degradation in the range 20 – 100 mT known as ‘Medium field Q-slope’. Understanding the origin of this phenomenon is important, in particular to future CW applications where cryogenic costs dictate the permissible cavity power and the Q-value determines the gradient. Previous studies on medium field Q-slope have been conducted by many authors, and models include hysteresis losses due to “strong-links” formed on the niobium surface during oxidation [1], energy gap decreasing due to superfluid motion [2], and mainly “global thermal instability” [3], [4], [5]. Here the heat created at the interior surface of the cavity, if not efficiently conducted to the low temperature bath, can increase the temperature of the rf surface. The surface resistance, which depends exponentially on the temperature, will rise increasing the power deposition leading to a further increase of the surface temperature. This effect strongly depends on the properties of the niobium and of the interface to the He bath, usually modelled through the RF surface resistance R_s , thermal conductivity k and kapitza conductance H_k . Medium field Q slope can be, in this thermal instability case, represented by a dimensionless parameter Γ introduced by Halbritter [3], defined via an expansion of the surface resistance R_s in even powers of the peak surface magnetic field B :

$$R_s(B) = R_{so} \left[1 + \gamma \left(\frac{B}{B_c} \right)^2 + O(B)^4 \right] \quad (1)$$

Here B_c is the thermodynamic critical field of niobium and R_{so} is the surface resistance at small magnetic fields. However, for our (and many other real) cavities a power series of R_s also contains odd powers of B , as we will discuss later. While medium field Q-slope studies have mainly been conducted for cavities operating at bath temperatures below 2.18K, in this paper we explore the effect for 141 MHz quarter wave cavities, at 4.2K. First we present ISAC-II quarter wave characterization curves. Then, experimentally we add two small resistive heaters on the cavity surface in contact with the 4.2K bath, in different peak magnetic field regions. This experiment aims to correlate an enhanced thermal feedback to the resulting Q slope, to test the thermodynamic limiting magnetic field and to study the effect of the Nb-He interface in the nucleate pool boiling regime. The experiment is done at 4.2K and 2K, and on different cavities. A model based on combination of thermal feedback and reduction of critical temperature with the RF field is then introduced. The temperature increase of the RF surface due to the heater power is directly measured using a test niobium chamber. The experimental results are then compared to the previously presented numerical model.

CHARACTERIZATION CURVES FITTING WITH HALBRITTER MODEL

From equation (1) we obtain the following expression for the decrease of the quality factor in terms of medium field Q slope:

$$Q(B) = \frac{G}{R_{so}} \left[1 - \gamma \left(\frac{B}{B_c} \right)^2 + O(B)^4 \right] \quad (2)$$

Fig. 1 shows characterization an example of Q-curves for three different 141 MHz TRIUMF BCP treated quarter wave cavities and the relative best fitting curves based on (2). A linear fit of the Q curves is also shown, which hints to the presence of a odd power term of $R_s(B)$ in addition to a quadratic. These results are consistent among the other ISAC-II quarter wave cavities.

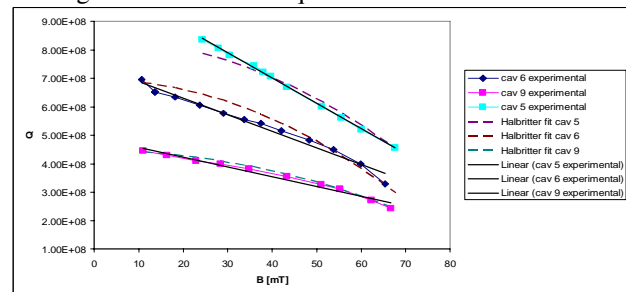


Figure 1: TRIUMF quarter wave cavities characterization curves and relative fit using Halbritter quadratic model and linear fit.

HEATERS TEST

To investigate the thermal dependence of the medium field Q-slope, we place two resistive heaters on the cavity surface in contact with the He bath. The heaters are placed in different peak magnetic field regions, one on the top of the inner conductor (maximum peak field) and one 20 cm down. They are both Polyimide resistive heaters, of values 75Ω and radii 20mm. The Nb wall thickness is 2 mm in each case. Initial checks are done by powering the resistors and monitoring He flow through a gas meter. These calibration curves are used to estimate the percentage of power going to the bath versus the one going actually into the Nb since the time constants are different. A low field ($H_p=20\text{mT}$) is established in the cavity and the heater power is increased. Several characterization curves at different heater power levels are then taken.

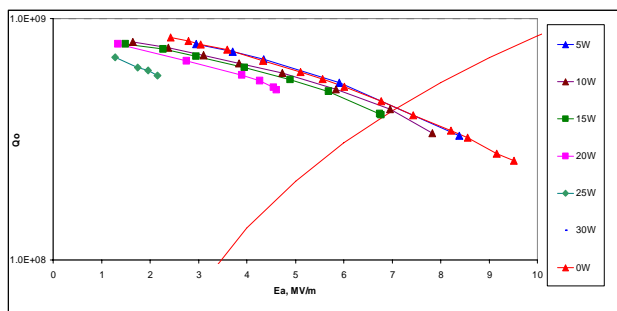


Figure 3: Example of Q curves at different heater power levels. The heater is placed on the top of the inner conductor surface of ISAC-II cavity 5, in contact with the He bath. Cavity wall is 2 mm thick.

The results shown in figure 3 are for a heater placed on the top part of the inner conductor; as expected, an increase in the heater power reduces the quench field points; however only as the heater value increases to 25 W the Q-slope is slightly increased. For the heater placed in lower magnetic field region (about half of the peak value) the quench points still decrease with the power, however all the curves overlap, so no significant change in Q-slope is found. The same result occurs for both top and bottom heater cases if the test is run at 2K.

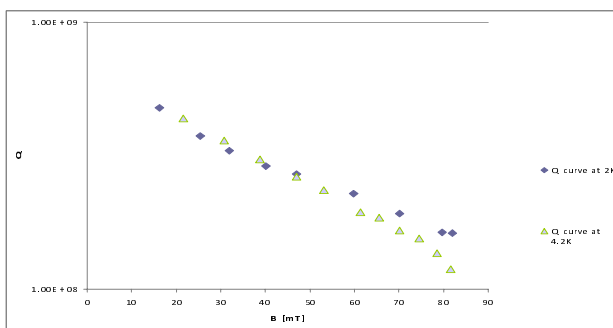


Figure 4: Q curves at 4.2 and 2K for ISAC-II cavity 15. Q curves at increasing heater power levels show early quenches but slope stays unchanged.

It is interesting though to compare the two Q-curves at 2K and 4.2K. As shown in figure 4, the two curves overlap at low field, meaning that the Q is dominated by a high residual resistance. However, the curves start separating at high field. This shows that the component of the surface resistance which carries the field dependence is the one that carries also the temperature dependence, likely the BCS component.

It is interesting then to plot and investigate the quench points due to different heater power levels. Quench points for top and bottom heater, at 4.2K and 2K are plot in the following graphs.

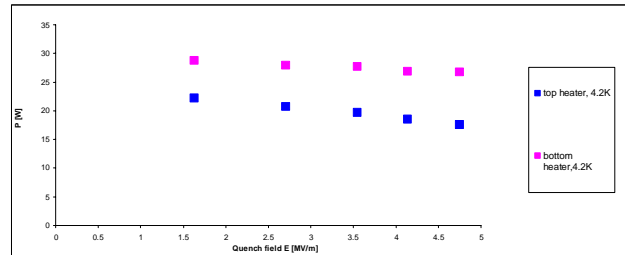


Figure 5a: Quench points at different power levels at 4.2K for heaters placed in different peak magnetic field regions of the inner conductor.

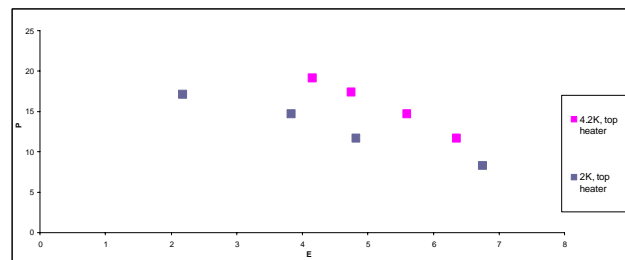


Figure 5b: Quench points at different power levels at 4.2K and 2K for heater placed on top part of the inner conductor.

THERMAL MODEL AND NUMERICAL SOLUTION

The idea behind our test is to enhance thermal feedback and correlate it to an eventually enhanced slope. Let's then approach the problem from the thermal point of view, and try to prove the theory right or wrong. Considering the cavity wall as an infinite flat slab of Nb of thickness d , the heat transmission problem becomes one-dimensional. The heat equation is:

$$P/A = -\kappa(T) \frac{dT}{dz} \tag{3}$$

where at the Rf surface:

$$P/A = \frac{1}{2} R_s(T) H^2 \tag{4}$$

and at the Nb-He interface $T_d = T_{\text{bath}} + \Delta T$, where ΔT involves the interface Kapitza conductance H_k . Expressions for H_k can be found in [6]. As we will discuss later, we also build a niobium test chamber to try to measure the temperature drop at the interface He-metal at 4.2K. The niobium slab can be divided into a series of small layers

producing a set of finite-difference equations. An important step is the choice of the surface resistance to use in equation (4).

Surface Resistance and Critical Temperature

A review of models of the RF surface resistance in high gradient Nb cavities can be found in [7]. There are several field dependent contributions to Rs, but for now we will simply consider the main components:

$$Rs(T) = Ro + R_{BCS}(T) \quad (5)$$

where Ro is the residual resistance due to impurities. R_{BCS} is due to the motion of normal electrons near the RF surface and can be calculated from the BCS theory of superconductivity, but has a rather complicated form. We will use a Pippard approximation:

$$R_{BCS} = 2.78 \times 10^{-5} \frac{v^2}{t} \ln\left(\frac{148t}{v}\right) \exp\left[-\frac{1.81g(t)}{t}\right] \quad (6)$$

where:

$$t = \frac{T}{T_c}, v = \frac{f}{2.86GHz}, g(t) = \left[\cos\left(\frac{\pi^2}{2}\right)\right]^{1/2} \quad (7)$$

Now, another key step is including or not the field dependence of the critical temperature T_c:

$$T_c(H) = 9.2 \sqrt{1 - (H/H_c)^2} \quad (8)$$

which takes into account, from the thermodynamic model, that the critical temperature is lowered in the presence of a RF field. Substituting (8) in (7) leads to a field dependence of the BCS resistance from the applied RF field.

Geometry of the Problem

We treat our problem considering a niobium disk of height equal to the thickness of the wall and radius given by that of the heater, as shown in Fig. 5. We assume that the edge of the disk is fixed at the bath temperature. The heat flows radially outward through the lateral surface of the disk, and the problem become one-dimensional, a fair approximation since the radius of the heater is 10 times larger than the thickness of the wall.

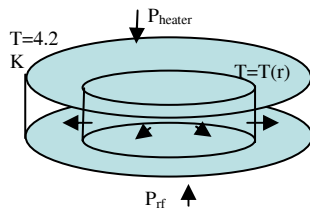


Figure 6: Schematic of the model. Heat coming from the Rf power and from the heater power flows across the lateral surface of the niobium disk. The edge of the disk is assumed at 4.2K.

We then divide the heater-sized disk into n disks and solve for the equilibrium temperature T(r). The heat flow transport is brought into a finite difference equation, with

two sources of heat: the heater power entering the metal, which is uniformly distributed across the disk and RF power, which is not uniform since disks with smaller radii will be at a higher temperature, therefore higher Rs. The temperature at every disk is then computed as:

$$T(r_i) = T(r_{i-1}) + \frac{P_{enclosed i}}{2\pi r_i \cdot d \cdot k(r_i)} \Delta r \quad (9)$$

$$P_{enclosed i} = \sum_1^i P_{RFi} + \alpha P_{heater} \cdot \frac{r_i^2}{a^2}$$

where d is the thickness of the wall, Δr is the radial extent of a ring, k is the thermal conductivity of Nb, α is the fraction of heater power entering the Nb and a is the radius of the heater.

NIBIUM TEST CHAMBER

In order to check our thermal model and also to get input parameters for the model (like heater power fraction going to Nb, temperature drop at the interface metal-Helium, etc...) we build a little Nb test chamber. The chamber hosts two Nb plates, each of thickness 2 mm BCP RRR=300 Niobium. The chamber inner surface is in He bath, and the outer in vacuum. On one side we place a heater in contact with the He bath and temperature sensors on the vacuum side and viceversa on the other side. This way we can achieve a direct measurement of the temperature increase of the surface due to the heater, and make a direct comparison with the values predicted by our model. The other side (heater in vacuum and T sensor in He bath) helps us investigating RF heating, and get measurements of the temperature drop at the interface He-metal. Experimentally this is a difficult measurement, as H_k is large at 4.2K and therefore ΔT is very small and difficult to measure accurately. A picture of the chamber and some results from the test are shown below.



Figure 7: Niobium test chamber. The temperature sensors shown are for direct measurement of temperature increase due to the heater placed on the other side of the 2 mm thick Nb plate.

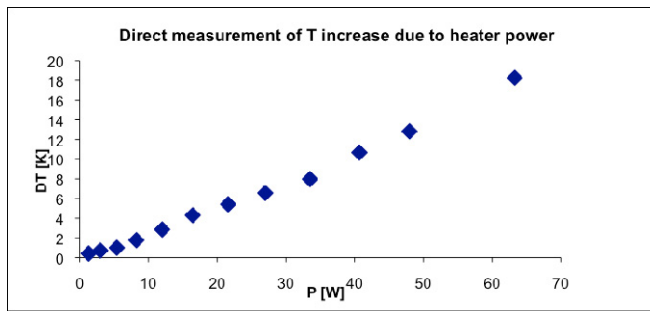


Figure 8: Measurement of T increase across 2mm thick Nb plate at different heater power levels.

EXPLAINING THE DATA

The quench condition corresponds to the field where the central temperature of the disk reaches T_c . Fig. 9 shows a plot of the heater power versus the quench field, comparing the experimental data with that of the model. The percentage of heater power entering the metal is used as a fitting parameter and it turns in close agreement with the transient analysis using the helium boil-off in the initial calibration and the Niobium chamber test. Several curves are shown. A result considering only RF thermal feedback, which means not taking into account (8), does not agree. Two other curves give reasonable agreement, one considering only the thermodynamic reduction of T_c with the applied field - which means simply looking at when $T(r=0)$ reaches the reduced critical temperature (8) - and another the thermodynamic model plus thermal feedback - which is looking for the quench computed taking into account thermal feedback with $R_{BCS}=f(H)$ through (8). The difference between those last two is small. The results seem to indicate a situation where the surface temperature does not increase unstably but rather exceeds the local critical temperature reduced by the RF field. Consequently, medium field Q slope might be dictated, more than by a RF driven thermal feedback, by the reduction of the critical temperature at increasing RF fields. And the small difference between thermodynamic model and thermodynamic plus thermal feedback is in agreement with the results of medium field Q-slopes not being enhanced at increasing heater power. These results are consistent for the bottom heater and 2K tests.

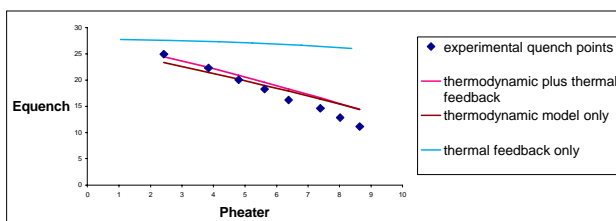


Figure 9: Comparison of experimental quench point at different heater power and the ones predicted by the model.

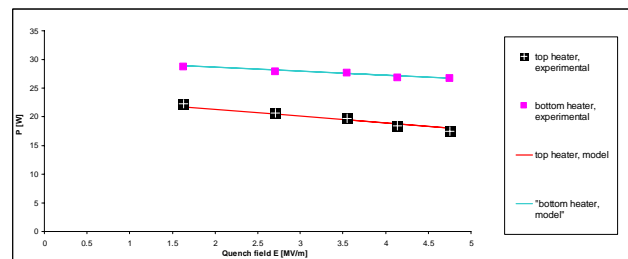


Figure 10: Good fit of the quench points is achieved for the top and bottom heater case taking into account the reduction of the critical temperature due to the presence of RF field.

CONCLUSIONS

The medium field Q-slope has been investigated for ISAC-II 141MHz quarter wave cavities. Characterization curves show both a linear and quadratic dependence on the peak magnetic field in the medium field range. Results of a heater test and comparison with a simplified heat transfer model seem to suggest a strong correlation between medium field Q slope and reduction of Nb critical T_c with the applied RF field. Comparison of Q curves at 2K and 4.2K shows that the temperature dependent component of the surface resistance is the one that carries the field dependence. From these conclusions, we are working on formulating a model for field dependent BCS resistance and compare it with Q curves of several cavities, operating at different frequencies and temperatures.

REFERENCES

- [1] G. Ciovati. Proceedings of the 12th International Workshop on RF Superconductivity, p230, TuP02, 2005.
- [2] V. Palmieri, The problem of Q drop in superconducting resonators, proceedings of SRF05 workshop.
- [3] J. Halbritter. RF residual losses, high electric and magnetic fields in superconducting cavities. Superconducting materials for high energy colliders, p.9, Eds Cifarelli and L.Maritato. World scientific, 1999.
- [4] K. Saito, Q slope analysis of Niobium SC RF cavities, proceedings of SRF workshop 2003.
- [5] J. Vines. Systematic Trends for the Medium Field Q-Slope, Proceedings of the 13th International Workshop on RF Superconductivity, TuP27, 2007.
- [6] Heat transfer and models for breakdown, H. Padamsee.
- [7] P. Bauer. Review of Models of RF Surface Resistance in High Gradient Niobium Cavities for Particle Accelerators.